Mechanism of carbon nanostructure synthesis in arc plasma

M. Keidar, A. Shashurin, O. Volotskova, Y. Raitses, and I. I. Beilis

Citation: Physics of Plasmas **17**, 057101 (2010); doi: 10.1063/1.3312879
View online: https://doi.org/10.1063/1.3312879
View Table of Contents: http://aip.scitation.org/toc/php/17/5
Published by the American Institute of Physics

Mechanism of carbon nanostructure synthesis in arc plasma[a)]

M. Keidar,[1,b)] A. Shashurin,[1] O. Volotskova,[1] Y. Raitses,[2] and I. I. Beilis[3]
[1]*George Washington University, Washington, DC 20052, USA*
[2]*Princeton Plasma Physics Laboratory, Princeton, New Jersey 08543, USA*
[3]*Tel Aviv University, Tel Aviv 69978, Israel*

(Received 15 December 2009; accepted 19 January 2010; published online 4 March 2010)

Plasma enhanced techniques are widely used for synthesis of carbon nanostructures. The primary focus of this paper is to summarize recent experimental and theoretical advances in understanding of single-wall carbon nanotube (SWNT) synthesis mechanism in arcs, and to describe methods of controlling arc plasma parameters. Fundamental issues related to synthesis of SWNTs, which is a relationship between plasma parameters and SWNT characteristics are considered. It is shown that characteristics of synthesized SWNTs can be altered by varying plasma parameters. Effects of electrical and magnetic fields applied during SWNT synthesis in arc plasma are explored. Magnetic field has a profound effect on the diameter, chirality, and length of a SWNT synthesized in the arc plasma. An average length of SWNT increases by a factor of 2 in discharge with magnetic field and an amount of long nanotubes with the length above 5 μm also increases in comparison with that observed in the discharge without a magnetic field. In addition, synthesis of a few-layer graphene in a magnetic field presence is discovered. A coupled model of plasma-electrode phenomena in atmospheric-pressure anodic arc in helium is described. Calculations indicate that substantial fraction of the current at the cathode is conducted by ions (0.7–0.9 of the total current). It is shown that nonmonotonic behavior of the arc current-voltage characteristic can be reproduced taking into account the experimentally observed dependence of the arc radius on arc current. © *2010 American Institute of Physics*. [doi:10.1063/1.3312879]

I. INTRODUCTION

Carbon nanostructures such as carbon nanotubes and graphene are continuing to enjoy much attraction due to their unique properties and great potential in various applications. Since the beginning of 1990s,[1] interest in carbon nanotubes has been stimulated by their unique mechanical, thermal and electrical properties, and various potential applications that exploit these properties. The most advanced applications of single and multiwall carbon nanotubes (MWNTs) include nanoelectronics,[2] field-emitters,[3] hydrogen storage,[4] biological and chemical gas sensors,[5] nanomaterials,[6] medicine,[7] etc.

Graphene, which is a single layer of carbon atoms, has attracted much attention recently because of its distinctive electronic properties (for example, high-carrier mobility).[8] Variety of unusual characteristic of graphene leads to its potential application in carbon-based electronics and magnetoelectronic devices.[9,10] Graphene plays an important role in experimental studies of basic properties of carbonate morphologies.[11–13] In recent years, a majority of graphene studies were focused on developing of methods of graphene production, namely, micromechanical exfoliation,[14] epitaxial growth on electrically insulating surfaces or by vapor deposition,[15,16] and thermal annealing.[17] A simple method of preparing graphene flakes by an arc discharge was described.[18] The synthesis procedure involved arc evaporation of graphite electrode in a hydrogen atmosphere. It was argued that presence of hydrogen terminated the dangling carbon bonds, thus preventing the formation of closed structures. In another recent work, an attempt was shown to synthesize graphene in an electric arc by employing a magnetic field.[19] It was suggested that nonuniform magnetic field affects precursor trajectories and energies to effect stacking of carbon atoms promoting carbon nanotubes and graphene growth.

Several advanced techniques were developed for carbon nanotube (CNT) synthesis such as arc discharge, laser ablation, and chemical vapor deposition.[20–22] Among plasma-based techniques for carbon nanostructure synthesis an arc discharge is probably the most practical from the both scientific and technological standpoints.[23,24] In fact, arc discharge technique has a number of advantages in comparison to other techniques[25] such as fewer defects and a high flexibility[26] of carbon nanostructures produced. Arc-grown nanotubes demonstrate the lowest emission capability degradation than those produced by other techniques.[27]

Typically, anodic arc is employed for synthesis of the carbon nanostructures. Exceptions are few works in which cathodic arc was used.[28] Anodic arc is characterized by primary anode ablation during the arc process in contrast to cathodic arc in which cathode ablation prevails.[29] When anodic arc is implemented for carbon nanotube synthesis it is supported by ablation of the anode material and substantial part of the ablated material (about 70%) is deposited on the cathode. Two different textures and morphologies can be observed in the cathode deposit; the gray outer shell and dark-soft inner core deposit. Post arc examination reveals that the MWNTs, as well as graphitic particles are found typically in

[a)]Paper GI2 6, Bull. Am. Phys. Soc. **54**, 94 (2009).
[b)]Invited speaker. Electronic mail: keidar@gwu.edu.

the inner core.[30] On the other hand single-wall carbon nanotubes (SWNTs) produced by the anodic arc discharge are found in a "collaret" around the cathode deposit, clothlike soot suspended in the chamber walls and the weblike structure suspended between cathode and walls.[30] In addition, the probability of MWNTs or SWNTs production in arc discharges dependents on gas background and arc conditions.[31,32] Issues related to large scale[33,34] and high purity synthesis of SWNT by arc discharge are very important objectives nowadays.[35–39]

Ability to control and tailor the synthesis process is one of the pressing issues. In this respect, the lack of control of the SWNT growth in an arc that is due to limited understanding of the arc physics and SWNT synthesis mechanism is the major disadvantage of this technique.[40] It is well-known that the arc plasma parameters can be controlled by a magnetic field[41] and, in fact, allows controlling the nanostructure production. Indeed it was shown that the high-purity MWNTs can be grown in the magnetically enhanced arc discharge[42] and that the magnetically enhanced arc leads to production of the long single-wall nanotubes.[43,44]

Although the mechanism of the formation and growth of SWNTs in an arc discharge was studied for a decade,[30] location of the region in an arc discharge in which SWNT synthesis occurs and the temperature range favorable for SWNT growth remains unclear. According to previous work,[30,45] the nanotube formation occurs on the periphery of an arc column at a moderate temperature range of 1200–1800 K. Other studies suggested that it is the cathode sheath adjacent to hot arc column ($\sim$5000 K) is the arc region where the nanotube growth occurs.[45–48] Recall that in the cathode sheath region, the temperature might be well above the reported critical temperatures of thermal stability of the nanotubes. In this respect, a question about possible carbon nanotube growth in cathode sheath region remains open. Moreover, there are no consistent data on the thermal stability of SWNT in the arc discharge, including the temperature ranges of SWNT synthesis and destruction.

In this paper, we summarize recent effort aiming to describe the entire phenomena associated with carbon nanotube synthesis including arc plasma, electrode erosion, carbon nanostructure synthesis, modeling, and postprocessing characterization of carbon nanotubes. Both experimental and theoretical efforts are described with overall objective to present the mechanism of synthesis of the carbon nanostructures in arc plasma. Recent experimental results led to better understanding the anode erosion mechanism,[49] current-voltage characteristics of the arc,[50] and cathode deposit mechanism.[51] Global model[52] developed by coupling anode erosion and interelectrode plasma phenomena is described. This model assists in understanding the arc plasma parameters associated with carbon nanotube synthesis and the controllability, as well as the efficiency of arc synthesis of the SWNTs.

The paper is organized as follows. Typical experimental setup, experimental results, and theoretical analysis of arc discharge plasma and SWNT thermal stability analysis are presented in Sec. II. Synthesis of carbon nanostructures including SWNTs and graphene is described in Sec. III. Description of plasma parameters associated with SWNT synthesis leading to strategy of localized control of SWNT production is addressed in Sec. IV.

II. PLASMA-ASSISTED SYNTHESIS IN ARC DISCHARGE

A. Arc discharge experimental study

Experiments are typically conducted in a cylindrical vacuum chamber (270 mm length and 145 mm diameter) filled with helium under pressure of about 500 Torr, as shown schematically in Figs. 1(a) and 1(b). The anode was attached to a linear drive system allowed to keep predetermined desired arc voltage. Arc was ignited by mechanical touching of arc electrodes (using anode feeding system) following by their immediate separation and was supported by welder power supply (Miller Goldstar 500ss). Arc electrodes were produced from carbon, with the anode being hollow tube and the cathode being solid. The cathode had a length and diameter of about 40 and 12.5 mm, respectively. The anode had a length of 75 mm before arcing (outer and inner diameters of the anode were 5 and 3.2 mm, respectively). The anode was packed with metal catalysts—Ni and Y in proportion Ni:Y=4:1. Nearly axial magnetic field in the interelectrode gap was produced by permanent magnet located near the arc electrodes (up to 1.5 kG).

Arc and weblike structures deposited on the cathode were photographed using digital camera [see Figs. 1(c) and 1(d)]. One can see that arc plasma has a sharp boundary that is determined by plasma-helium gas interface interactions. Below, we will discuss significance of the plasma boundary considerations. Weblike structure shown in Fig. 1(d) represents primary source of SWNT synthesized in arc discharge.

B. Arc characteristics

Primary focus of arc discharge study was voltage-current (*V-I*) characteristics (see experimental data in Fig. 4). Without the presence of magnetic field, *V-I* characteristics had V-type shape with point of minimum shifting to higher arc currents with gap length increase (from about 25 A in the case of 2.5 mm gap to about 45 A in the case of 13 mm gap length).[50] Increase in interelectrode gap also led to shift in entire characteristic to higher voltages (voltage increase in about 20 V in the case of gap length increase from 2.5 to 13 mm). With presence of magnetic field *V-I* characteristic demonstrated similar V-shaped behavior, while the point of minimum (I_{cr} is the arc current that corresponds to minimum voltage) was shifted toward the higher arc currents (approximately tens of amperes) in comparison to that obtained at the same arc conditions without magnetic field.[50] *V-I* characteristics with and without magnetic field were close for arc currents larger than I_{cr}, while for smaller current, arc was unstable and was apt to interrupt.

C. SWNT thermal stability study

Recently, the thermal stability of SWNTs produced in at helium arc was studied.[53] Using a furnace, we were able to create temperature conditions (for SWNT sample), closely

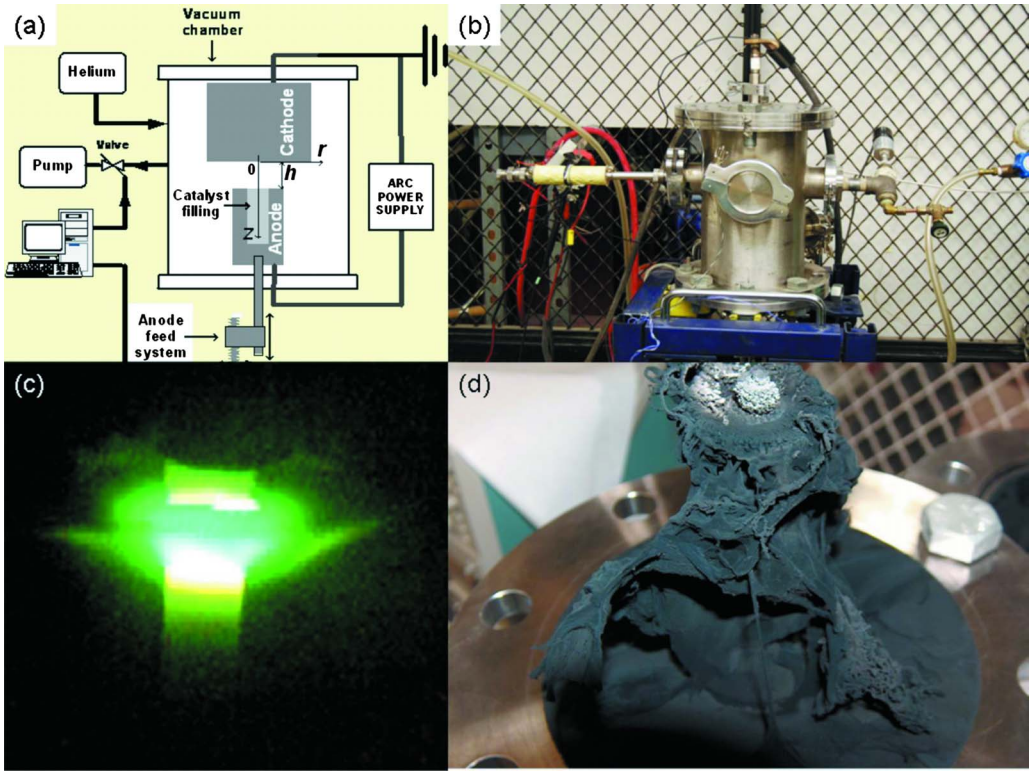

FIG. 1. (Color online) (a) Schematics of the arc discharge, (b) photo of the experimental setup, (c) typical photograph of the arc, and (d) image of the collected nanotube web.

resembling the natural conditions of SWNT growth in an arc. The electrical resistance of SWNT sample was analyzed at different helium pressures, as well as in vacuum as shown in Fig. 2. Abrupt increase in the sample resistance corresponds to nanotube ignition and subsequent destruction (Ref. 53).

According to these results, the temperature conditions of arc SWNT synthesis correspond to a maximum temperature T_{cr}, which is below 1100 K. Based on this result, one can estimate the characteristic time needed for SWNT, being heated by plasma of arc column to reach this critical temperature. Using a simplified analysis, the energy balance can be formulated as follows: $C_{\mathrm{SWNT}}M_{\mathrm{SWNT}}(\Delta T/\Delta t)=Q_{pl}$, where C_{SWNT} and M_{SWNT} are the heat capacitance and mass of SWNT and Q_{pl} is the heat flux from the plasma to the SWNT surface (radiation from the SWNT surface is neglected). The heat flux from the plasma to individual SWNTs (nanotubes are at floating potential, i.e., $|j_e|=|j_i|$) can be estimated as

$$Q_{pl}=j_i\left(2T_e+T_e\ln\sqrt{\frac{M}{m}}\right)A,$$

where j_i is the current density from the plasma to the SWNTs, A is the SWNT collecting area, and M and m are the masses of carbon atom and electron, respectively. Assuming that the maximum time is the time necessary to reach temperature T_{cr}, one can obtain that time required for SWNT destruction in an arc column, which is about 10 μs (for plasma density of about 10^{13} cm^{-3}, $T_e=1$ eV). In the above estimation lowest possible plasma density was used and therefore it gives upper limit of destruction time and thus the destruction time in an arc column might be less than 10 μs. We can compare the estimated time for SWNT destruction with time of SWNT flight through the arc plasma column. The lower bound estimate of time of flight can be obtained using a high SWNT velocity of about 10^3 cm/s (Ref. 40) and this led to about 1 ms for typical size of plasma column of about 1 cm. The comparison of these times yields that time of destruction is much smaller than the time of flight across the discharge area clearly indicating that SWNTs generated anywhere inside the arc most likely would not be able to survive during their transport though the column. Thus, maximum temperature determined from electrical resistance

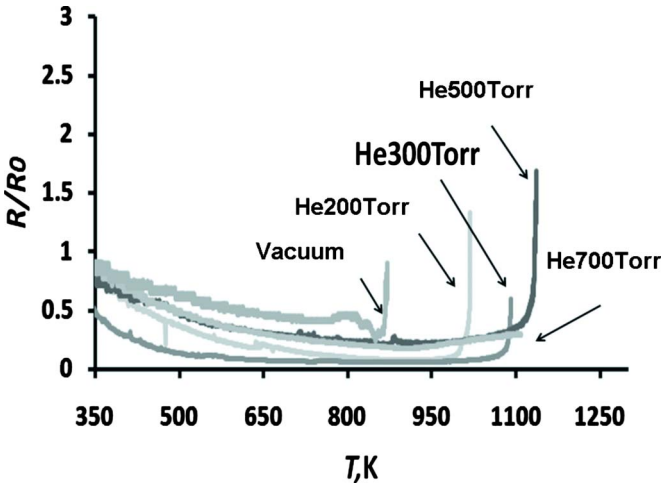

FIG. 2. (Color online) Resistance of SWNT network as a function of temperature with helium pressure as a parameter.

measurements combined with SWNT dynamics analysis can be used for predicting SWNT synthesis region. Based on the above estimation, it can be suggested that SWNT produced by an anodic arc discharge and collected in the web area outside the arc plasma most likely originated from the arc discharge peripheral region, i.e., plasma-gas interface. This results is in agreement with previous studies[44–46] that considered that region of formation of SWNT is restricted by the temperature range of about 1200–1800K.

D. Enhancement of carbon supply. Effect of the anode geometry

The anode ablation rate is critical to understanding the arc operation as a whole because the anode provides the plasma ions, and eventually the raw material for carbon nanotube production. In recent experiments with the atmospheric pressure helium arc,[49] the ablation rate of a graphite anode was investigated as a function of the anode diameter. For the sake of this study no metal catalysts were used in the arc, and thus, ablation rate of graphite only was determined. For an anodic arc with the ablating anode, the existing theoretical models predict the electron-repelling (negative) anode sheath. Under such conditions, the peak ablation rate of the graphite anode is expected to occur when the anode diameter is equal to the arc channel diameter. However, it was found that anomalously high ablation occurs for small anode diameters (<0.4 cm).[49] This result was explained by the formation of an electron-attracting (positive) anode sheath leading to increased power deposited by electrons on small anodes as compared with larger anodes.[49] The increased ablation rate due to this positive sheath could imply a greater yield of carbon nanotube production. It was suggested that plasma convergence as the mechanism for the positive anode sheath formation. More details of the arc plasma modeling are discussed in Sec. II E.

E. Theoretical study of arc discharge plasma

The purpose of the arc plasma discharge model is to obtain plasma parameters of the discharge relevant for carbon nanotube synthesis, which is very difficult to measure. For the sake of simplicity, we present here a global coupled plasma-electrode model of an anodic discharge, which has the main features describing the phenomena related to the interelectrode plasma, thermal regime of the electrodes, current continuity at the electrodes, and to the anode erosion rate. Carbon species are supplied by anode erosion which is determined by the anode temperature. In turn, anode temperature is affected by the heat flux from the interelectrode plasma which is controlled by plasma density. It was observed that the erosion of the cathode is negligible during the arcing.[50–52] Carbon species interact with helium atmosphere and this interaction ultimately determines the dynamic boundary of the arc.

Plasma state in the interelectrode gap of the arc is determined by the energy balance[54]

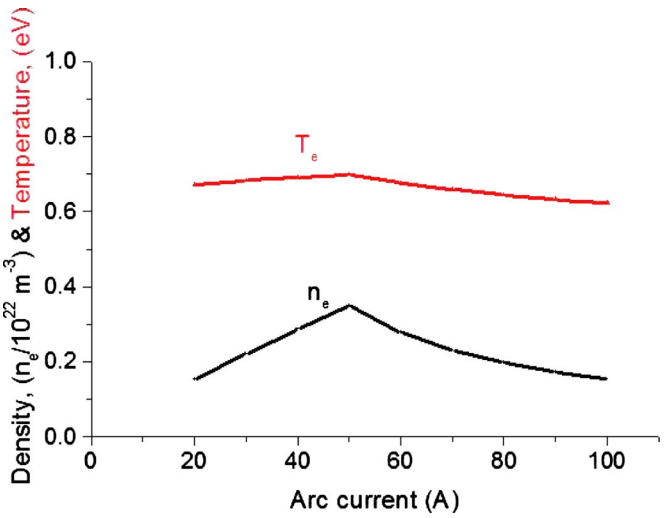

FIG. 3. (Color online) Calculated electron density and temperature as a function of the arc current.

$$I_{\mathrm{arc}}U_{pl} + U_c I_e = I_{\mathrm{arc}}(2T_e + U_a) + U_{iz}I_{\mathrm{ion}} + 3\frac{m_e}{m_i}(T_e - T_a)n_e\nu_e\pi R_{\mathrm{arc}}^2 L_{\mathrm{gap}}, \quad (1)$$

where I_{arc} is the arc current, I_e is the electron current at the cathode, U_{pl} is the potential drop in the interelectrode gap, U_c is the cathode voltage, I_{ion} is the ion current at the cathode, T_e is the electron temperature, U_a is the anode voltage, U_{iz} is the ionization potential of carbon, R_{arc} is the arc radius, L_{gap} is the interelectrode gap length, n_e is the electron density in the interelectrode gap, T_e is the electron temperature, ν_e is the electron collision frequency, and T_a is the neutral temperature. In this equation the left-hand side term is Joule heating, while right-hand side terms are heat losses to the anode, losses due to ionization and heat transfer from electrons to neutral species. It is assumed that heavy particles (ions and neutrals) are in equilibrium and have the temperature, which is equal to anode temperature. The full system of equation includes current conservation at the cathode and anode, energy balance at the cathode and anode, and Saha equation for plasma composition. Detailed model is described in a recent publication (Ref. 52).

Recall that it was found that one of the important characteristics of the interelectrode plasma in arc discharge is the arc radius variation with arc current.[51] The arc radius dependence on arc current can be approximated as

$$R_{\mathrm{arc}} = R_a(\alpha I_{\mathrm{arc}}), \quad I_{\mathrm{arc}} \geq 50 \text{ A}, \qquad R_{\mathrm{arc}} = R_a, \quad I_{\mathrm{arc}} < 50 \text{ A}, \quad (2)$$

where $\alpha = 0.02$ is a coefficient obtained from experiments.[51,52] It should be pointed that in the framework of the global model of the discharge arc radius dependence on the current has significant effect on the discharge and plasma parameters. For instance, the electron temperature and electron density initially increases with arc current, as it is shown in Fig. 3. This dependence can be explained by increase in the power deposition into the plasma (Joule heat-

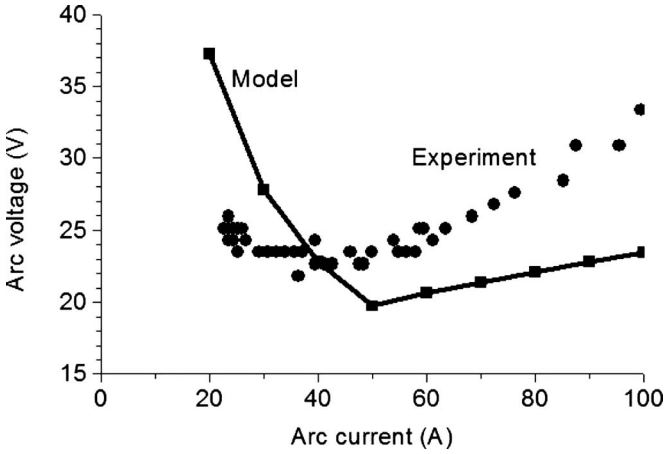

FIG. 4. Calculated voltage-current characteristics of the arc discharge and comparison with experimental data (Refs. 50 and 52).

ing) with increase in the arc current. When arc discharge current increases above the about 50 A, arc radius increases leading to increase in the plasma volume. In turn, this leads to a decrease in the electron temperature, plasma density, and ionization fraction in the interelectrode gap. These calculations suggest that arc plasma is characterized by electron temperature of about 0.6–0.7 eV and electron density of about 10^{21} m^{-3}.

Calculated voltage-current characteristic of the arc discharge is shown in Fig. 4. One can see that calculated arc voltage initially decreases with arc current, reaches the minimum and then increases. Such trend is generally in agreement with experimental data, as shown in Fig. 4 for comparison. It should be pointed out that nonmonotonic behavior of the arc voltage displayed in Fig. 4 is the result of cathode voltage dependence on the arc current as described above and therefore is a direct consequence of model condition that arc radius increases with arc current (for $I>50$ A).

Thus, modeling of the arc discharge leads to conclusion that in order to describe properly arc discharge physics, one needs to take into account coupling between processes in interelectrode plasma and electrodes, current continuity at electrodes, and thermal regime of electrodes. Another important conclusion of the model is that the nonmonotonic behavior of the arc voltage can be only reproduced by considering arc radius dependence on the arc current.

III. SYNTHESIS OF CARBON NANOSTRUCTURES

Arc plasma can be used as a platform for synthesis various carbon nanostructures including MWNT, SWNT, and graphene. Below, the synthesis of SWNT and recently discovered graphene structures are considered.

A. SWNT

SWNTs are considered the main product of arc discharge synthesis due to their superior properties in comparison to SWNTs grown by other techniques.[25] Based on the observation of the arc during the synthesis (see Sec. II A), as well as on the studies of the thermal stability of the SWNT (see Sec. II B), it is apparent that the primary synthesis region is the plasma boundary, i.e., arc plasma-helium interface. This result led to several approaches for control of the SWNT synthesis including the application of an electric field (Ref. 40) and a magnetic field (Ref. 43).

Recall that previous models suggested several scenarios for SWNT growth termination in arc discharge (Ref. 40). These scenarios are related to the mechanism of carbon species precipitation. However, in addition, it was shown that SWNT synthesis is coupled with SWNT dynamics and formation time. The SWNT gains a kinetic energy due to momentum transfer from plasma and leave the plasma region having conditions which are optimal for synthesis.[40] Thus, increasing the SWNT residence time in the region of synthesis can be suggested as a possible way for SWNT synthesis control. One possibility to increase SWNT residence time is the electrostatic trapping taking into account that SWNTs are charged. Simulations[40] predicted that very large ratios of the SWNT length to radius (aspect ratio) are possible by application of the electric field of about few V/m in the region of synthesis. On the other hand it was experimentally demonstrated that magnetic field leads to significant increase in the average SWNT length with maximum length increase by a factor of 5 and average length increase by a factor of 2 in comparison to the synthesis without magnetic field.[43,44] This effect was explained by increase in the plasma density (due to plasma focusing) and related to that increase in the SWNT growth rate.

It is accepted that SWNTs are created by rolling up a hexagonal lattice of carbon (graphite). Rolling the lattice at different angles creates a visible twist or spiral in the SWNT's molecular structure, though the overall shape remains cylindrical. This twist is called chirality. SWNTs are characterized by chirality in addition that their diameter and length.[12] The SWNT's chirality, along with its diameter, determines its electrical properties. The armchair structure has metallic characteristics. Both zigzag and chiral structures produce band gaps, making these nanotubes semiconductors. Thus, dependent on chirality SWNT can have metallic or semiconductor conductivity. Ultraviolet visible and near-infrared absorbance spectra are standard ways to characterize SWNT chirality structure.[55] Typical spectra of SWNT as-grown sample are shown in Fig. 5. Intensity of the peak is proportional to SWNT electronic structure. One can see that most arc produced SWNTs have semiconductor conductivity (about 70%), while about 30% nanotubes are metallic. Inset transmission electron microscope (TEM) image of SWNT grown in arc discharge conditions is also shown in Fig. 5. One can see that both single nanotubes and bundles are synthesized in arc plasma.

It is important to make a comment on preferable synthesis of the SWNT in arc discharge in which SWNT are synthesized in the plasma volume in contrast with surface based synthesis leading to primarily MWNT formation.[56] Previous simulations[56] suggested several possible modes of SWNT formation dependent on the ratio of SWNT or catalyst particle size to the Debye length. It was shown that in all cases, SWNT growth in the plasma volume is accompanied by strong carbon ion flux to the SWNT seed and catalyst. The strong ion flux to the metal catalyst particle leads to the two

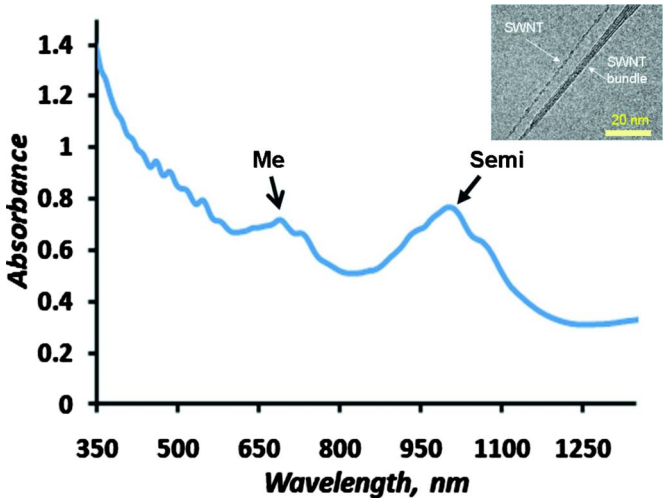

FIG. 5. (Color online) Typical absorbance spectra of SWNT as-produced sample. Inset shows TEM image of SWNT grown in arc discharge conditions.

main effects: first, it provides effective conditioning and heating of the catalyst particle; second, it supplies a large amount of carbon material for the nanotube growth.[56] It was suggested that these effects promote growth of SWNT in plasma volume of the arc discharge.[40,56]

B. Graphene

Recently it was found that few-layer graphene particles can be growth in an arc plasma controlled by a magnetic field.[57] Variety of diagnostics including scanning electron microscope (SEM), TEM, Raman, and atomic force microscopy (AFM) was used to identify the single or few-layer graphene particles.[57] Figure 6 shows SEM and AFM imaging of the samples collected from magnet sides and indicate presence of graphene flakes on the magnet. Estimated size of sheets is in the order of 0.1–1 μm. AFM has been of the most reliable methodology to identify single and few layers of graphene flakes.[58] AFM image [Fig. 6(b)] displays the in-plane dimensions (upper image) and height (lower image) of the graphene nanostructure. Figure 6(b) shows the presence of flake structures with surface size of around a micron and a height variation of 1–2 nm with respect to a mica surface and occurrence of "bumps/wrinkles" with its height variation about 0.5 nm similar to that found previously for graphene.[58] Based on these results it can be concluded that arc plasma allow to synthesis of a few-layer graphene particles. These results are very promising, opening new robust way for synthesis of this novel and distinct material.

IV. DIAGNOSTICS OF THE SWNT SYNTHESIS REGION

Our preliminary experimental and theoretical studies suggest that SWNT and graphene synthesis occurs at the interface between the arc plasma and helium (see Sec. II). Therefore study of the plasma parameters and SWNT collection in this region is of particular importance.

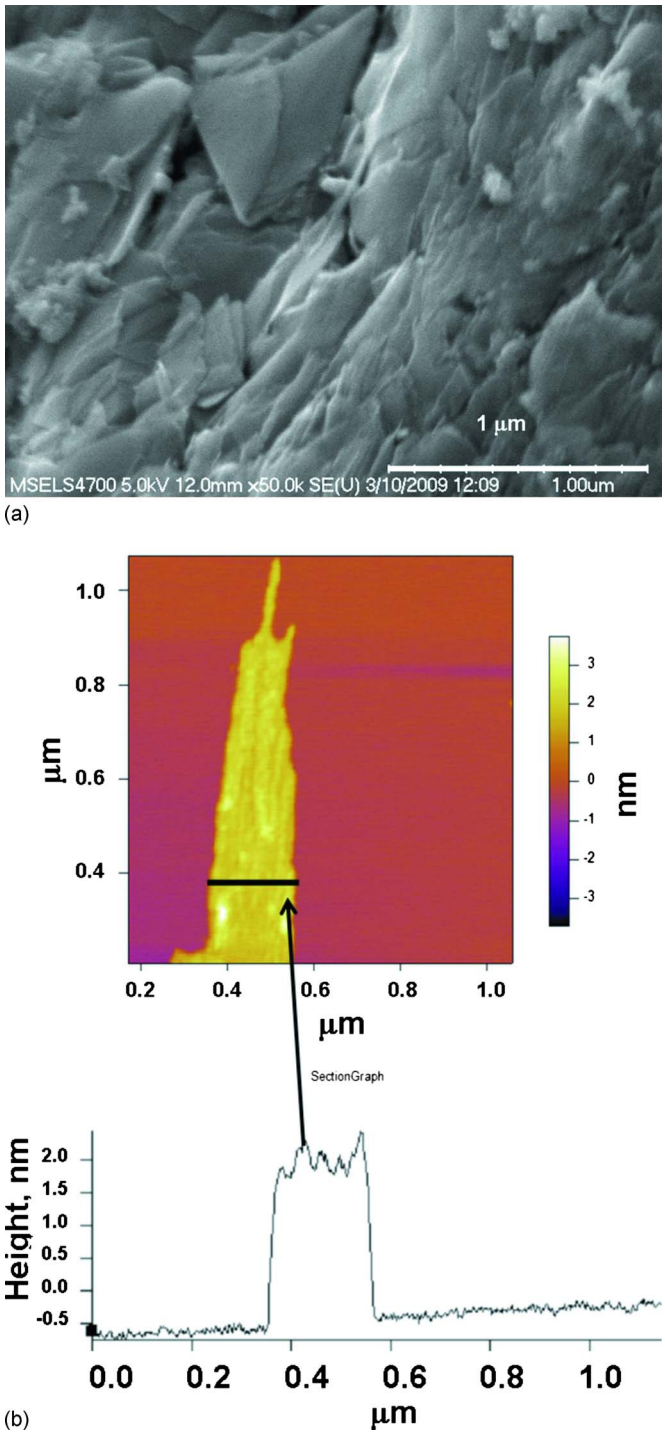

FIG. 6. (Color online) Imaging of samples collected from the magnet side: (a) SEM and (b) AFM.

A. Experimental study of plasma-helium interface

For the local plasma parameter diagnostics, we used probe equipped with fast moving shutter (controlled by solenoid) in order to limit time of probe exposition to the plasma flux. Probe consists of a thin W-wire (0.5 mm in diameter) installed inside the ceramic tube (alumina with outside diameter of 6.3 mm) with opening of about 5×3 mm^2. The cylindrical shutter (made of a rolled molybdenum sheet) is closely fitted to the outside surface of the ceramic tube and

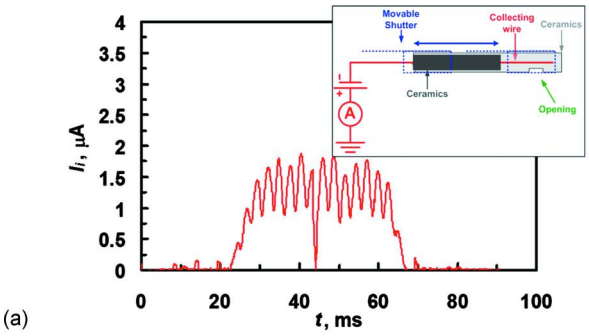

(a)

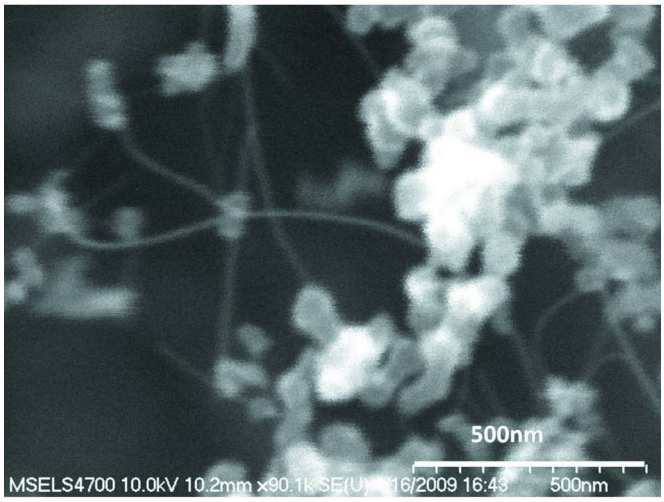

(b)

FIG. 7. (Color online) Current collected by probe. Inset shows the schematics of the probe (a) and SEM image of SWNT deposited on small probe (b).

able to slide along it. Shutter position is controlled using electrically driven solenoid and W-wire is exposed to the plasma only during shutter open time. The schematic view of the probe is presented on the inset of Fig. 7(a). The probe is movable and can be placed at various radial positions. In the described below experiments the probe was placed at the plasma-helium interface. This is the region of preferable SWNT growth according to our estimations (see Sec. II). The distance to the arc was about 7 mm and the probe bias was about −50 V with respect to cathode.

Nonzero current from plasma (about 1.5 μA for case of the arc current of about 55 A) was detected when shutter was open [see Fig. 7(a)]. Probe also collected SWNTs during the shutter opening. Typical SEM of the collected SWNTs is shown in Fig. 7(b) confirming that probe collected SWNTs. In the next section, we will discuss consequences of current collection from plasma containing significant amount of SWNTs.

Recall that probe operation in carbon plasma is not a trivial procedure since any probe immersed in the carbon environment is significantly contaminated.[50] In this respect, probe having a fast moving shutter as described above proved to be robust technique for plasma and SWNT local diagnostics.

B. Analysis of SWNT motion and probe collection

With respect to the plasma and SWNT diagnostics by a biased probe a following question can be posed: can the collected SWNT flux provide significant current exceeding electron and ion currents under certain conditions? The model of SWNT probe collection was developed recently.[59] The main issue of the model is accounting for SWNT charging in the vicinity of probe. In this study it was assumed that probe is placed in the quasineutral plasma, so that the steady state sheath formation time (which is approximately scales as an ion flight time across the sheath) is much smaller than the voltage sweep time. The model takes into account that SWNT are formed in the vicinity of the plasma-sheath interface and, therefore, SWNT enters the sheath with zero charge. It was assumed that the SWNT charging occurs in the sheath considering SWNT interaction with ions and electrons in the sheath. According to this model, the calculations were preformed for the following conditions: SWNT radius and length are 1.5 nm and 10 μm, respectively, electron temperature and density are 0.6–0.7 eV and $(1-2)\times 10^{16}$ m^{-3}, respectively.[60]

It was found that when probe is biased positively with respect to the plasma boundary, SWNTs entering sheath are charged to a negative charge and are attracted to the biased probe. Charging in the sheath is enhanced in comparison with the charging in quasineutral plasma due to ion density decrease in the positive sheath. In the case of a negatively biased probe the situation becomes more complicated. Due to electron depletion in the sheath, SWNT moving across the sheath are charged positively and can carry a positive charge to the probe forming the current of opposite polarity in comparison with the current in the case of a positively biased probe. According to the calculations,[59] it was concluded that current collected from SWNT-contained plasma might be determined by the SWNT flux in both cases of positively and negatively biased probe. In addition, it follows that the collected current by the SWNT charge flux maybe of the same order of magnitude in both negatively and positively biased probe. Recall that this conclusion is correct if electron density charge in the plasma, i.e., Zen_e is about $n_{SWNT}Q_{SWNT}$, where Z and e are ionicity and electron charge, n_{SWNT} and Q_{SWNT} are the density and charge of SWNTs in plasma bulk, respectively. In this case, current collected by the probe is determined by the current transferred by SWNT flux due to SWNT charging in the sheath.

V. CONCLUDING REMARKS

This paper outlined basic issues related to synthesis of carbon nanostructures in arc discharge. Given that among plasma-based techniques, arc discharge stands out as very advantageous in several ways (fewer defects, high flexibility, and longer lifetime); this techniques warrants attention from the plasma physics standpoint. It was demonstrated in experiment and theoretically that controlling plasma parameters can affect nanostucture synthesis altering SWNT properties (length and potentially, chirality) and leading to synthesis of new structures such as a few-layer graphene. Among clearly identified parameters affecting synthesis are

magnetic and electric fields. Knowledge of the plasma parameters and discharge characteristics is crucial for ability to control synthesis process by virtue of both magnetic and electric fields.

Theoretical analysis suggests that in order to describe arc physics properly, one needs to take into account coupling between processes in interelectrode plasma and electrodes, current continuity at electrodes, and thermal regime of electrodes. Important feature that should be accounted for is the arc radius increase with the arc current according to experimental observation. In fact, it was concluded that the nonmonotonic behavior of the arc voltage can be only reproduced by considering arc radius dependence on arc current.

In spite of a decade long history of intense research, some basic understanding of the region of SWNT formation in arc discharge is still unknown and subject of controversy. Recent idealized experiment was conducting aiming to establish the temperature range for SWNT favorable growth conditions. Based on these measurements, it can be suggested that SWNT produced by an anodic arc discharge and collected in the web area outside the arc plasma most likely originate from the arc discharge peripheral region, i.e., plasma-gas interface. As result, it was suggested the idea of localized collection and control of SWNT growth. In fact, preliminary results support the proposed idea and demonstrated possibility of SWNT collection at the plasma-helium interface region.

ACKNOWLEDGMENTS

This work was supported in part by NSF/DOE Partnership in Plasma Science and Technology (NSF Grant No. CBET-0853777 and DOE Grant No. DE-SC0001169). We would like to acknowledge PPPL Offsite Research Program supported by Office of Fusion Energy Sciences for supporting arc experiments.

[1] S. Iijima, Nature (London) **354**, 56 (1991).
[2] W. H. Chiang and R. M. Sankaran, Nature Mater. **8**, 882 (2009).
[3] A. Buldum and J. P. Lu, Phys. Rev. Lett. **91**, 236801 (2003).
[4] H. Gao, X. B. Wu, Ji. T. Li, G. T. Wu, J. Y. Lin, K. Wu, and D. S. Xu, Appl. Phys. Lett. **83**, 3389 (2003).
[5] J. Kong, N. R. Franklin, C. Zhou, M. G. Chapline, S. Peng, K. Cho, and H. Dai, Science **287**, 622 (2000).
[6] T. Tersoff, Phys. Rev. B **46**, 15546 (1992).
[7] J. Gao and B. Xu, Nanotoday **4**, 37 (2009).
[8] K. S. Novoselov, A. K. Geim, S. V. Morozov, D. Jiang, M. I. Katsnelson, I. V. Grigorieva, S. V. Dubonos, and A. A. Firsov, Nature (London) **438**, 197 (2005).
[9] Y. Zhang, Y.-W. Tan, H. L. Stormer, and P. Kim, Nature (London) **438**, 4235 (2005).
[10] S. Pisana, M. Lazzer, C. Casiraghi, K. S. Novoselov, A. K. Geim, A. C. Ferrari, and F. Mauri, Nature Mater. **6**, 198 (2007).
[11] D. V. Kosynkin, A. L. Higginbotham, A. Sinitskii, J. R. Lomeda, A. Dimiev, B. K. Price, and J. M. Tour, Nature (London) **458**, 872 (2009).
[12] M. S. Dresselhaus, G. Dresselhaus, and P. C. Eklund, *Science of Fullerence and Carbon Nanotubes* (Academic, New York, 1996).
[13] A. Gupta, G. Chen, P. Joshi, S. Tadigadapa, and P. C. Eklund, Nano Lett. **6**, 2667 (2006).
[14] K. S. Novoselov, D. Jiang, F. Schedin, T. J. Booth, V. V. Khotkevich, S. V. Morozov, and A. K. Geim, Proc. Natl. Acad. Sci. U.S.A. **102**, 10451 (2005).
[15] E. V. Rutkov and A. Ya. Tontegode, Surf. Sci. **161**, 373 (1985).
[16] C. Berger, Z. Song, T. Li, X. Li, A. Y. Ogbazghi, R. Feng, Z. Dai, A. N. Marchenkov, E. H. Conrad, P. N. First, and W. A. de Heer, J. Phys. Chem. B **108**, 19912 (2004).
[17] T. Ohta, F. El Gabaly, A. Bostwick, J. L. McChesney, K. V. Emtsev, A. K. Schmid, T. Seyller, K. Horn, and E. Rotenberg, New J. Phys. **10**, 023034 (2008).
[18] K. S. Subrahmanyam, L. S. Panchakarla, A. Govindaraj, and C. N. R. Rao, J. Phys. Chem. C **113**, 4257 (2009).
[19] S. Karmakar, N. V. Kulkarni, A. B. Nawale, N. P. Lalla, R. Mishra, V. G. Sathe, S. V. Bhoraskar, and A. K. Das, J. Phys. D **42**, 115201 (2009).
[20] Z. Huang, J. Xu, Z. Ren, J. Wang, M. Siegal, and P. Provencio, Appl. Phys. Lett. **73**, 3845 (1998).
[21] U. Cvelbar, B. Markoli, I. Poberaj, A. Zalar, L. Kosec, and S. Spaić, Appl. Surf. Sci. **253**, 1861 (2006).
[22] F. J. Gordillo-Vázquez, V. J. Herrero, and I. Tanarro, Chem. Vap. Deposition **13**, 267 (2007).
[23] C. Journet, W. K. Maser, P. Bernier, A. Loiseau, M. L. de la Chapelle, S. Lefrant, P. Deniard, R. Lee, and J. E. Fischer, Nature (London) **388**, 756 (1997).
[24] K. Ostrikov, Rev. Mod. Phys. **77**, 489 (2005).
[25] *Carbon Nanotubes: Science and Applications*, edited by M. Meyyappan (CRC, Boca Raton, 2004).
[26] I. Stepanek, G. Maurin, P. Bernier, J. Gavillet, A. Loiseau, R. Edwards, and O. Jaschinski, Chem. Phys. Lett. **331**, 125 (2000).
[27] Y. Okawa, S. Kitamura, and Y. Iseki, Proceedings of the Ninth Spacecraft Charging Technology Conference, Japan, April 2005 (unpublished).
[28] H. Takikawa, M. Yatsuki, T. Sakakibara, and S. Itoh, J. Phys. D **33**, 826 (2000).
[29] I. I. Beilis, IEEE Trans. Compon. Packag. Technol. **23**, 334 (2000).
[30] A. P. Moravsky, E. M. Wexler, and R. O. Loufty, in *Carbon Nanotubes: Science and Applications*, edited by M. Meyyappan (CRC, Boca Raton, 2004).
[31] S. Farhat, M. L. De La Chapelle, A. Loiseau, C. D. Scott, S. Lefrant, C. Journet, and P. Bernier, J. Chem. Phys. **115**, 6752 (2001).
[32] E. I. Waldorff, A. M. Waas, P. P. Friedmann, and M. Keidar, J. Appl. Phys. **95**, 2749 (2004).
[33] Y. Y. Ando, X. Zhao, K. Hirahara, K. Suenaga, S. Bandow, and S. Iijima, Chem. Phys. Lett. **323**, 580 (2000).
[34] T. Zhao and Y. Liu, Carbon **42**, 2765 (2004).
[35] I. Levchenko, K. Ostrikov, M. Keidar, and S. Xu, Appl. Phys. Lett. **89**, 033109 (2006).
[36] X. Lv, F. Du, Y. Ma, Q. Wu, and Y. Chen, Carbon **43**, 2020 (2005).
[37] D. Tang, L. Sun, J. Zhou, W. Zhou, and S. Xie, Carbon **43**, 2812 (2005).
[38] M. Yao, B. Liu, Y. Zou, L. Wang, D. Li, T. Cui, G. Zou, and B. Sundqvist, Carbon **43**, 2894 (2005).
[39] M. Keidar and A. M. Waas, Nanotechnology **15**, 1571 (2004).
[40] M. Keidar, J. Phys. D **40**, 2388 (2007).
[41] M. Keidar, I. I. Beilis, R. L. Boxman, and S. Goldsmith, J. Phys. D **29**, 1973 (1996).
[42] K. Anazawa, K. Shimotani, C. Manabe, H. Watanabe, and M. Shimizu, Appl. Phys. Lett. **81**, 739 (2002).
[43] M. Keidar, I. Levchenko, T. Arbel, M. Alexander, A. M. Waas, and K. Ostrikov, Appl. Phys. Lett. **92**, 043129 (2008).
[44] M. Keidar, I. Levchenko, T. Arbel, M. Alexander, A. M. Waas, and K. Ostrikov, J. Appl. Phys. **103**, 094318 (2008).
[45] M. Keidar, Y. Raitses, A. Knapp, and A. M. Waas, Carbon **44**, 1022 (2006).
[46] S. Farhat and C. D. Scott, J. Nanosci. Nanotechnol. **6**, 1189 (2006).
[47] I. Hinkov, J. Grand, M. L. de la Chapelle, S. Farhata, J. B. Clement, C. D. Scott, L. B. Johnson, P. Nikolaev, V. Pichot, and P. Launois, J. Appl. Phys. **95**, 2029 (2004).
[48] E. G. Gamaly and T. W. Ebessen, Phys. Rev. B **52**, 2083 (1995).
[49] A. Fetterman, Y. Raitses, and M. Keidar, Carbon **46**, 1322 (2008).
[50] A. Shashurin, M. Keidar, and I. I. Beilis, J. Appl. Phys. **104**, 063311 (2008).
[51] A. Shashurin and M. Keidar, Carbon **46**, 1826 (2008).
[52] M. Keidar and I. I. Beilis, J. Appl. Phys. **106**, 103304 (2009).
[53] O. Volotskova, A. Shashurin, M. Keidar, Y. Raitses, V. Demidov, and S. Adams, Nanotechnology **21**, 095705 (2010).
[54] I. I. Beilis, R. L. Boxman, and S. Goldsmith, Phys. Plasmas **9**, 3159 (2002).
[55] J. A. Fagan, B. J. Landi, I. Mandelbaum, J. R. Simpson, V. Bajpai, B. J. Bauer, K. Migler, A. R. Hight Walker, R. Raffaelle, and E. K. Hobbie, J. Phys. Chem. B **110**, 23801 (2006).

[56]I. Levchenko, K. Ostrikov, M. Keidar, and U. Cvelbar, J. Phys. D **41**, 132004 (2008).
[57]O. Volotskova, I. Levchenko, A. Shashurin, Y. Raitses, K. Ostrikov, and M. Keidar, "In situ magnetic separation of freestanding graphene and nanotubes in arc plasma," Nano Lett. (to be published).
[58]H. C. Schniepp, J.-L. Li, M. J. McAllister, H. Sai, M. Herrera-Alonso, D. H. Adamson, R. K. Prudhomme, R. Car, D. A. Saville, and I. A. Aksay, J. Phys. Chem. B **110**, 8535 (2006).
[59]M. Keidar and I. I. Beilis "On a model of nanoparticle collection by an electrical probe," IEEE Trans. Plasma Sci. (to be published).
[60]M. Keidar, A. M. Waas, Y. Raitses, and E. Waldorff, J. Nanosci. Nanotechnol. **6**, 1309 (2006).